

Reversal of Momentum Relaxation

G. A. Melkov, Yu. V. Kobljanskyj, A. A. Serga, and V. S. Tiberkevich
Radiophysical Faculty, National Taras Shevchenko University of Kiev, Kiev, Ukraine

A. N. Slavin

Department of Physics, Oakland University, Rochester, Michigan 48309

(Received 25 January 2001)

A new phenomenon of *momentum relaxation reversal* has been discovered experimentally and explained theoretically for dipolar spin waves in magnetic garnet films. It is shown that the process of momentum relaxation, caused by the scattering of a signal wave on defects, can be reversed, and the signal can be restituted *after* it left the scattering region. The reversal of momentum relaxation is achieved by frequency-selective parametric amplification of a narrow band of scattered waves having low group velocities and frequencies close to the frequency of the original signal wave. The phenomenon can be used for the development of a new type of active microwave delay lines.

DOI: 10.1103/PhysRevLett.86.4918

PACS numbers: 75.30.Ds, 76.50.+g, 85.70.Ge

Dissipation of waves and oscillations in any real medium is usually happening as a result of thermodynamic relaxation processes when the energy of oscillations and waves is irreversibly transferred to a thermal reservoir, statistical and thermodynamic equilibrium is established, and entropy of the system is increased.

There are, however, examples of relaxation processes that are reversible, at least during a certain time interval. All such reversible relaxation processes have a common property: the energy of the input signal of the frequency ω_s is initially distributed among a large number of oscillations (or waves) having different amplitudes $c_{\mathbf{k}}$ and eigenfrequencies $\omega_{\mathbf{k}}$, which in a general case are randomly distributed around the signal frequency ω_s . After the signal is switched off at the moment $t = 0$ all these oscillations, which previously were oscillating at the signal frequency ω_s , start to oscillate at their own eigenfrequencies $\omega_{\mathbf{k}}$. As a result, the individual phases of these oscillations become random with time, and the system quickly undergoes a transition to a totally “dephased” state. During this process the relative phase shifts of the oscillators $\phi_{\mathbf{k}} = (\omega_{\mathbf{k}} - \omega_s)t \equiv \Delta\omega_{\mathbf{k}}t$ continuously increase with time. In this dephased state the macroscopic signal, which is a result of interference of all individual oscillations, vanishes after a characteristic dephasing time T^* , which can be much shorter than the characteristic time of irreversible energy relaxation T [1,2]. Thus during the time interval $T^* < t < T$ the relaxation is still reversible, and the original signal can be restituted.

One of the examples of a reversible relaxation process is the process of *phase relaxation* that is responsible for the effects of spin and photon echo [1,2]. In this case the macroscopic signal in the medium can be restored, at least partially, by the operation of phase conjugation (or time reversal) [2] performed during the time interval $T^* < t < T$. These operations result in a “phasing” (opposite to “dephasing”) process in which the phase shifts

$\phi_{\mathbf{k}}$ decrease with time until the system is “in-phase” again, and the macroscopic polarization is restored.

In this paper we report the first experimental observation and theoretical interpretation of a *new method* of signal restoration from a dephased state of individual oscillations (or waves) created at the initial stages of a signal relaxation. We demonstrate that the macroscopic signal can be restored by *frequency-selective amplification* of waves (or oscillations) having frequencies close to the frequency of the initial signal $\Delta\omega_{\mathbf{k}} \equiv \omega_{\mathbf{k}} - \omega_s \simeq 0$. This new process does not involve phase conjugation or time reversal operations traditionally used for the reversal of phase relaxation [1,2].

The scheme of the proposed process is shown in Fig. 1. After the initial stage of wave relaxation the system is in a dephased state (Fig. 1a), where wave amplitudes $c_{\mathbf{k}}$ are approximately equal, phase shifts $\phi_{\mathbf{k}} = (\omega_{\mathbf{k}} - \omega_s)t \equiv \Delta\omega_{\mathbf{k}}t$ are distributed evenly, and the macroscopic signal (equal to the vectorial sum of all the vectors $c_{\mathbf{k}}$) is zero.

We propose to apply to the dephased waves in this system a frequency-selective amplification with the gain $G(\Delta\omega_{\mathbf{k}})$ that is inversely dependent on the frequency difference $\Delta\omega_{\mathbf{k}}$. The waves having smaller phase

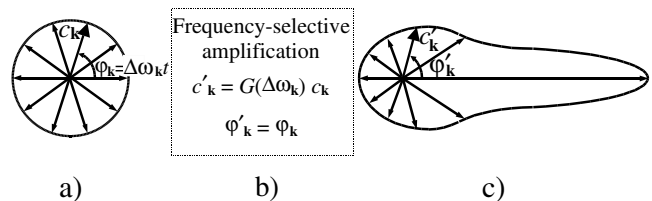


FIG. 1. Restoration of a macroscopic signal from a dephased state by means of a frequency-selective amplification: (a) symmetric dephased state of a large number of waves (oscillations) created at the initial stage of the input signal relaxation; (b) strong frequency-selective amplification of waves having small phase shifts $\phi_{\mathbf{k}} \simeq 0$; (c) asymmetric state of the system after frequency-selective amplification.

shifts $\phi_{\mathbf{k}} = (\omega_{\mathbf{k}} - \omega_s)t \equiv \Delta\omega_{\mathbf{k}}t$ will experience much stronger amplification than the waves with larger phase shifts (Fig. 1b). Thus, the symmetry of the energy distribution among the waves having different phase shifts will be broken, and the interference of these amplified waves will result in the appearance of a nonzero macroscopic signal at the output (see Fig. 1c). The frequency-selective amplification necessary for the proposed new relaxation reversal process can be realized by different methods and, in particular, by means of a narrow-band parametric amplification (see, e.g., [3] and Chap. 10 in [4]).

The proposed method of relaxation reversal by frequency-selective amplification can be used not only for the reversal of phase relaxation [1,2] but also for the reversal of any other reversible relaxation process. In this paper we used frequency-selective amplification to demonstrate for the first time the reversal of a *wave vector (or momentum) relaxation*.

The process of wave vector (or momentum) relaxation is well known in physics. As a result of this process, the energy of a spectrally narrow signal wave packet, which is initially concentrated near the signal carrier wave vector \mathbf{k}_s , is distributed over a much wider region of \mathbf{k} space due to the signal scattering on inhomogeneities (or defects) in the medium. A well-known example of such a process is the scattering of light in a frosted glass or in any other matte medium.

One of the brightest manifestations of the momentum relaxation process can be observed in magnetically ordered crystals where this process is known as *nonintrinsic two-magnon relaxation process* caused by the scattering of spin waves on static inhomogeneities and defects (see Chap. 11 in [4]). This process gives the main contribution to the observed linewidth of nonhomogeneous magnetostatic precession modes and long-wave ($k_s \leq 10^2 \text{ cm}^{-1}$) dipolar spin waves (magnetostatic waves) in magnetic crystals. The properties of dipolar spin wave spectrum are such that not only the direction but also the magnitude of the spin wave vector is changed in the scattering process, while the wave frequency remains almost constant (see Chap. 7 in [4]).

As a result of the two-magnon scattering, the original (signal) spin wave having wave vector \mathbf{k}_s excites relatively short spin waves having wave vectors \mathbf{k} with magnitudes $k \approx |k_s \pm 2\pi/a| \approx 10^4 \text{ cm}^{-1}$, where $a \sim 1 \text{ }\mu\text{m}$ is the size of the defect which caused scattering. These short spin waves created in the scattering process have low group velocities ($v_{\mathbf{k}} \ll v_s$). Therefore, these short spin waves remain near the defect and can interact with it during a relatively long time interval after the signal wave had passed the defect and left the scattering region.

The interaction of a signal wave with defects is usually linear and reciprocal. Thus, the short spin wave with the wave vector \mathbf{k} , localized near the defect and oscillating with its own eigenfrequency $\omega_{\mathbf{k}}$ (which is not exactly equal to the signal frequency ω_s), can interact again with the de-

fect and generate a wave with the wave vector \mathbf{k}_s . The interference of these secondary signal “generators” will not result, however, in the restitution of the original signal. The time-dependent phase shifts of all the secondary generators $\phi_{\mathbf{k}} = (\omega_{\mathbf{k}} - \omega_s)t \equiv \Delta\omega_{\mathbf{k}}t$ will be different, and the averaged macroscopic signal will be zero.

To check experimentally the possibility of momentum relaxation reversal by means of frequency-selective amplification we performed experiments on the system of dipolar spin waves propagating along the direction of the constant bias magnetic field \mathbf{H}_0 in a tangentially magnetized yttrium-iron garnet (YIG) film sample (backward volume magnetostatic waves). We have chosen parametric amplification with pumping frequency twice larger than the signal carrier frequency $\omega_p = 2\omega_s$ as a method of frequency-selective amplification of scattered waves. In addition to high and well-controlled frequency selectivity of amplification this method preserves the phases of amplified waves (see Chap. 5 in [3]).

In our experiments we used a conventional delay line (Fig. 2) consisting of an input (1) and output (2) microstrip transducers of the width $50 \text{ }\mu\text{m}$ separated by the distance 5 mm . An additional pumping microstrip transducer (3) of the width $200 \text{ }\mu\text{m}$ was placed in the middle. This transducer arrangement was previously used in the experiments on parametric amplification of linear spin wave pulses and solitons in YIG films [5,6]. A YIG film sample (thickness $d = 30.3 \text{ }\mu\text{m}$, in-plane sizes $1 \text{ mm} \times 20 \text{ mm}$, saturation magnetization $4\pi M_0 = 1750 \text{ Oe}$, bias magnetic field $H_0 = 1015 \text{ Oe}$, and ferromagnetic resonance linewidth $2\Delta H = 0.7 \text{ Oe}$) was placed on top of the structure.

A rectangular microwave signal pulse of the carrier frequency $\omega_s = 2\pi \times 4.7 \text{ GHz}$, duration $\tau_s = 50 \text{ ns}$, and power $P_s = 5 \text{ mW}$ was supplied to the input transducer and was propagating with group velocity $v_s = 13 \text{ cm}/\mu\text{s}$ in the YIG film sample. In the process of propagation the signal was scattered on the defects and inhomogeneities in the film. The pumping pulse of the carrier frequency $\omega_p = 2\omega_s = 2\pi \times 9.4 \text{ GHz}$, duration $\tau_p = 150 \text{ ns}$, and power $P_p = 5 \text{ W}$ was supplied to the pumping (middle) transducer Δt ns after the trailing edge of the signal pulse

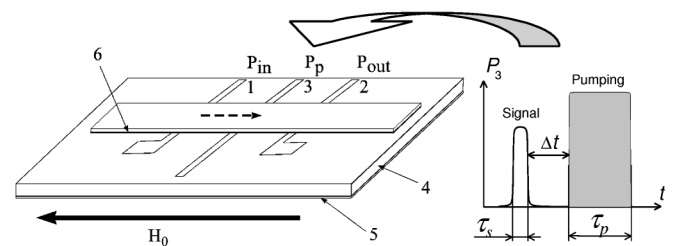


FIG. 2. Experimental setup: 1, 2, and 3—input, output, and pumping transducers; 4—dielectric substrate; 5—metal screen; 6—YIG film. The inset shows the signal and pumping pulse profiles at the pumping transducer (3). τ_s and τ_p are, respectively, the widths of the signal pulse and the pumping pulse; Δt is the time interval between the signal and pumping pulses.

left the pumping localization region. The inset in Fig. 2 shows the relative positions of the signal and pumping pulses at the pumping transducer (3). Microwave pumping magnetic field was created only in the immediate vicinity of the pumping transducer, so the direct interaction of the signal with pumping was excluded.

The results of our experiments are presented in Fig. 3. The inset in Fig. 3 shows the oscillogram of the signal at the output transducer. It can be seen that, besides the usual delayed and attenuated signal pulse (1), a new amplified and further delayed pulse (2) is observed. The magnitude and the time delay of this second pulse (2) are strongly dependent on the parameters of the microwave pumping pulse. We stress that this second pulse (2) appears at the output *only* if the primary signal pulse (1) had passed in the film before the pumping has been switched on. *The pumping alone does not generate this pulse.*

We believe that the pulse (2) is a restituted signal, resulting from the reversal of momentum relaxation of the original signal on the defects in the YIG film sample. The reversal is performed by means of parametric amplification of scattered short spin waves having the smallest values of frequency detuning relative to the signal $\Delta\omega_{\mathbf{k}} = (\omega_{\mathbf{k}} - \omega_s)$ (see Fig. 1).

The experimental data presented in the main part of Fig. 3 support this interpretation. The data points in the main part of Fig. 3 show the dependencies of the relative peak powers of the pulses (1) and (2) measured at the output transducer on the time delay Δt between the signal and pumping measured at the middle transducer (see the inset in Fig. 2). It can be seen that the usual signal (1) is not affected by pumping in any way, while the restituted signal (2) for small delays Δt is amplified by parametric

pumping to the amplitudes significantly (7 dB) larger than the amplitude of the usual signal (1). For the larger values of the delay time Δt the power of the restituted signal (2) decreases parabolically (in logarithmic scale) with the increase of Δt .

To prove the role of defects in the observed relaxation reversal process we increased the surface roughness of the YIG film sample by treating it with the diamond abrasive paste with the grain size of $3 \mu\text{m}$. The experimentally measured signal restitution coefficients $K(\Delta t) = P_{2\text{out}}/P_{1\text{out}}$ for smooth (A) and rough (B) film samples are presented in Fig. 4 (points). It can be clearly seen that the increase of surface roughness (and, therefore, of the number of defects causing two-magnon scattering) leads to the increase of the amplitude of the restituted signal by almost 10 dB at $\Delta t \approx 0$.

A simple theoretical model for the interpretation of the above described effect of *momentum relaxation reversal* is based on well-known equations for the two-magnon scattering process (see, e.g., [7] and Chap. 11 in [4]). We added to these equations an additional term containing the amplitude h_p of microwave pumping magnetic field and describing parametric amplification of scattered spin waves to get

$$\frac{\partial a_s}{\partial t} + i\omega_s a_s + \Gamma_s a_s = -i \sum_{\mathbf{k}} R_{\mathbf{k}} c_{\mathbf{k}}, \quad (1a)$$

$$\frac{\partial c_{\mathbf{k}}}{\partial t} + i\omega_{\mathbf{k}} c_{\mathbf{k}} + \Gamma_{\mathbf{k}} c_{\mathbf{k}} = -iR_{\mathbf{k}}^* a_s - iV_{\mathbf{k}} h_p e^{-i\omega_p t} c_{-\mathbf{k}}^*, \quad (1b)$$

where a_s and $c_{\mathbf{k}}$ are the amplitudes of the signal wave and scattered wave with wave vector \mathbf{k} , respectively; $\omega_{s,\mathbf{k}}$

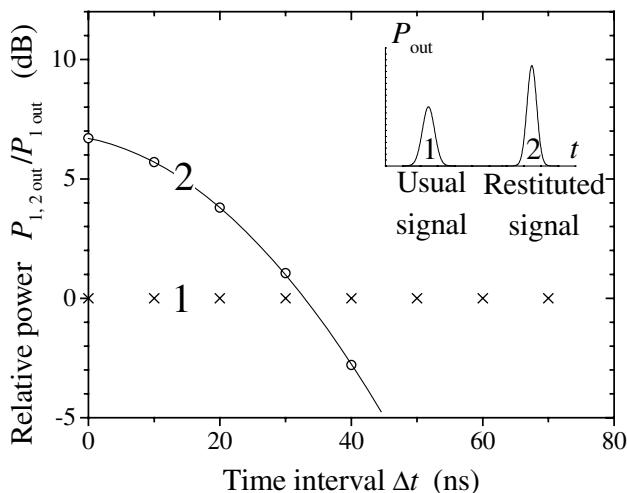


FIG. 3. Dependence of peak output powers of the usual (1) and restituted (2) signals on the time interval Δt between the signal and pumping pulses at the middle (3) transducer (see Fig. 2). Solid line—theoretical calculation using Eq. (3). The inset shows a schematic view of the oscillogram at the output antenna.

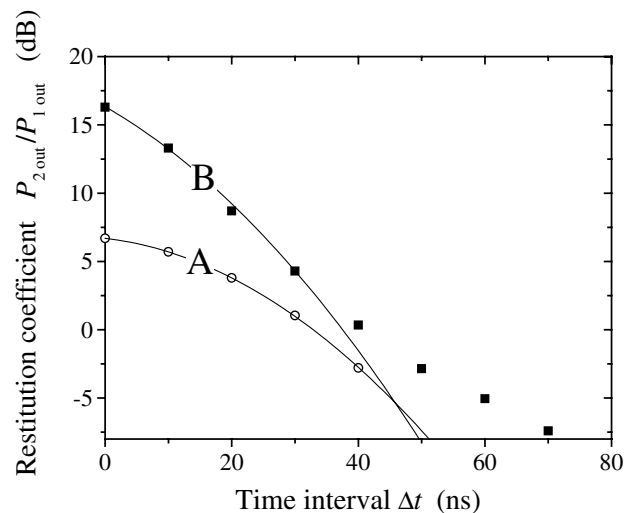


FIG. 4. Influence of the film surface roughening on the amplitude of the restituted spin wave signal [signal (2) in Fig. 3]: A—untreated (smooth) film; B—treated with abrasive (rough) film. Points—experiment; solid lines—theoretical calculation using Eq. (3).

and $\Gamma_{s,\mathbf{k}}$ are their frequencies and relaxation parameters, respectively; $R_{\mathbf{k}}$ is the scattering intensity of the signal wave into the wave $c_{\mathbf{k}}$; $V_{\mathbf{k}}$ is the coupling coefficient of the scattered waves with pumping defined by Eq. (4.3.20) in [3].

It follows from Eq. (1b) that the parametric pumping acts on the secondary spin waves $c_{\mathbf{k}}$ as a frequency-selective amplifier with the power gain [8,9]

$$G(\Delta\omega_{\mathbf{k}}) \equiv \left(\frac{c'_{\mathbf{k}}}{c_{\mathbf{k}}}\right)^2 \approx G_0 \exp[-(2\Delta\omega_{\mathbf{k}}/\Omega)^2], \quad (2)$$

where $G_0 = \exp[(V_{\mathbf{k}}h_p - \Gamma_{\mathbf{k}})\tau_p]/2$ is the resonant ($\Delta\omega_{\mathbf{k}} = 0$) parametric gain dependent on the pumping power and pumping pulse duration τ_p , while $\Omega = \sqrt{V_{\mathbf{k}}h_p/2\tau_p}$ is the frequency band of parametric amplification for the given parameters of the pumping pulse.

Assuming that the decay rates of both the signal wave and scattered waves are equal $\Gamma_s = \Gamma_{\mathbf{k}} \equiv \Gamma$ and that the input pulse duration τ_s is much smaller than the lifetime of waves $\tau_s \ll \Gamma^{-1}$, we derived an approximate expression for the signal restitution coefficient $K(\Delta t)$ defined as the ratio of the power of restituted signal to the power of usual signal at the output

$$K(\Delta t) \equiv \left(\frac{a'_s}{a_s}\right)^2 \approx K_0 \exp[-2(\Gamma\Delta t + \Omega^2\Delta t^2)], \quad (3)$$

where K_0 is the restitution coefficient corresponding to $\Delta t = 0$ and dependent on the input pulse duration, scattering intensity, and number of defects in the medium. It was assumed that P_{out} is proportional to $|a_s|^2$. It is clear from Eq. (3) that the theoretical restitution coefficient decreases parabolically (in a logarithmic scale) with Δt in good qualitative agreement with experiment (Figs. 3 and 4).

Calculated curves obtained using Eq. (3) are in reasonable quantitative agreement with the experiment for both untreated (smooth) and treated (rough) films (see solid curves in Figs. 3 and 4) if we assume that the theory and experiment in both cases coincide at $\Delta t = 0$. We used the following parameters of the model (3):

(A) untreated (smooth) film

$$\Gamma = 6.16 \times 10^6 \text{ s}^{-1} \quad (\Delta H_{\mathbf{k}} = 0.35 \text{ Oe});$$

(B) treated (rough) film

$$\Gamma = 30.4 \times 10^6 \text{ s}^{-1} \quad (\Delta H_{\mathbf{k}} = 1.73 \text{ Oe}).$$

The other parameter in Eq. (3) $\Omega/2\pi = 3.6 \text{ MHz}$ ($h_p = 33 \text{ Oe}$) is the same for both cases. The parameter values

used in our calculation in the case of untreated film are close to the experimental values of $\Delta H_{\mathbf{k}}$ and h_p obtained in our previous work on YIG films [5,8]. Thus, the simple expression (3) gives a good explanation of the experimental data, which provides a further support to our interpretation of the observed effect as a *reversal of momentum relaxation*.

The proposed method of relaxation reversal may find important practical applications in optical, radio-frequency, and microwave signal processing. The parametric amplification process in a microwave range used in our experiments is very effective and can provide amplification gains of up to 30 dB [6,9]. Thus, the signal could be restituted to measurable amplitudes a relatively long time (about several microseconds) after the relaxation of the original signal took place. The proposed process of active relaxation reversal can be used to develop a new type of active microwave delay lines. The delay time in such a line is proportional to the time interval Δt (see Fig. 2) and is determined by the moment when the pumping pulse is supplied. For the pumping power $P_p < 10 \text{ W}$ the delay time may vary in the interval from zero to several microseconds and is easily controlled.

In conclusion, we proposed a new method of relaxation reversal by means of a frequency-selective amplification of secondary waves created in the relaxation process of the original signal. This method is applicable to any kind of reversible relaxation process. Using this method, we demonstrated for the first time the *reversal of momentum relaxation* of waves in the media with stationary defects.

This work was supported by NSF Grant No. DMR-0072017 and by CRDF Grant No. UP1-2120.

-
- [1] A. Abragam, *The Principles of Nuclear Magnetism* (Clarendon, Oxford, 1961).
 - [2] J. C. Au Yeung, in *Optical Phase Conjugation*, edited by R. A. Fisher (Academic Press, New York, 1983), Chap. 9.
 - [3] V. S. L'vov, *Wave Turbulence Under Parametric Excitation* (Springer, Berlin, Heidelberg, 1994).
 - [4] A. G. Gurevich and G. A. Melkov, *Magnetization Oscillations and Waves* (CRC Press, New York, 1996).
 - [5] A. V. Bagada, G. A. Melkov, A. A. Serga, and A. N. Slavin, *Phys. Rev. Lett.* **79**, 2137 (1997).
 - [6] P. A. Kolodin *et al.*, *Phys. Rev. Lett.* **80**, 1976 (1998).
 - [7] M. Sparks, *Ferromagnetic Relaxation Theory* (McGraw-Hill, New York, 1964).
 - [8] G. A. Melkov *et al.*, *Phys. Rev. Lett.* **84**, 3438 (2000).
 - [9] G. A. Melkov *et al.*, *Sov. Phys. JETP* **89**, 1189 (1999).